JOURNAL OF GEOPHYSICAL RESEARCH, VOL. 106, NO. D14, PAGES 15,065–15,075, JULY 27, 2001

Ice particles in stratiform clouds in the Arctic and possible mechanisms for the production of high ice concentrations

Arthur L. Rangno and Peter V. Hobbs

Department of Atmospheric Sciences, University of Washington, Seattle

Abstract. The presence of ice particles in clouds affects precipitation processes, the radiative properties of the clouds, and the derivation of cloud properties from remote sensing measurements. High ice particle concentrations occur often in slightly to moderately supercooled clouds in the Arctic. This paper combines data collected in a common type of ice-producing arctic cloud (stratocumulus) with calculations based on laboratory experiments to elucidate mechanisms that might be responsible for the ice. Ice splinters produced during riming could account for the relatively high concentrations of ice particles in clouds that encompass temperatures between –2.5°C and –8°C. However, it has generally been assumed that ice splinters grow into pristine ice crystal habits, whereas detailed measurements in an arctic stratocumulus cloud showed that only 32% of the ice particles were pristine crystals (needles, sheaths, short columns, and plates) and 10% were broken pieces of needles or sheaths. Thirty-seven percent of the ice particles were not identifiable crystal types, 20% were frozen drops, and 1% were aggregates and graupel. The large numbers of unidentifiable ice particles could have originated from the fragmentation of delicate ice crystals and the shattering of some drops during freezing in free fall. These two mechanisms may also play a role in the production of relatively high ice particle concentrations in moderately supercooled arctic clouds that lie outside of the temperature zone where ice splinter production by riming occurs.

1. Introduction

Clouds play a dominant role in the radiation balance of the Arctic [e.g., *Curry et al.*, 1993, 1996]. Correct understanding and numerical model simulations of the radiative effects of clouds, and the formation of precipitation, require information on cloud structures and processes. Also, the remote sensing of cloud properties is sensitive to cloud structures [*Mishchenko et al.*, 1996; *Hobbs et al.*, this issue].

Relatively few in situ measurements on the structures of arctic clouds are available. Perhaps the most comprehensive study reported is that of *Hobbs and Rangno* [1998] who described airborne measurements of the microstructures of low- and middle-level stratiform clouds over the Beaufort Sea obtained in April 1992 and early June 1995. One of the most interesting conclusions of this study was that temperature alone is not a very good predictor of ice particle concentrations in slightly to moderately supercooled stratiform clouds in the Arctic.

As part of the First ISCCP Regional Experiment–Arctic Cloud Experiment/Surface HEat Budget of the Arctic Ocean (FIRE-ACE/SHEBA) field study, the University of Washington (UW) Convair-580 aircraft flew 23 missions (totaling 97 research hours) over the Arctic Ocean between May 19 and June 24, 1998. The cloud measurements obtained in these studies provide extensive documentation on the structures of arctic clouds and an opportunity to explore the mechanisms responsible for these structures. As in our 1995 studies [*Hobbs and Rangno*, 1998], we found that ice particles are common in arctic clouds that are only slightly to moderately supercooled (Figure 1).

In this paper, information is provided on the types and concentrations of ice particles in slightly to moderately supercooled arctic stratiform clouds. This information is then used to assess the possible roles of several mechanisms that have been proposed for the formation of relatively high ice particle concentrations in slightly to moderately supercooled clouds.

2. Synoptic Situation and Flight Pattern

We will focus on a case study that is typical of slightly supercooled stratiform clouds in the Arctic and for which extensive data was collected. The data for this case study were collected from the UW Convair-580 research aircraft from ~2000 to 2300 UTC (1300-1600 Alaska daylight time) on June 2, 1998, over the ice-covered Arctic Ocean near Barrow, Alaska. During this period there was a weak low-pressure center and an upper level short wave trough to the west of Barrow. These produced advancing multilayered clouds to the southwest of a line of broken to scattered stratocumulus cloud in which the airborne measurements were obtained. The stratocumulus cloud produced heavy virga, some of which may have reached the ground as light rain showers. There was no visible cloud above the stratocumulus, and no ice crystals, which form at temperatures below -6°C (e.g., stellars, dendrites, bullet rosettes), were detected either within or above the stratocumulus layer.

Paper number 2000JD900286.
0148-0227/01/2000JD900286$09.00

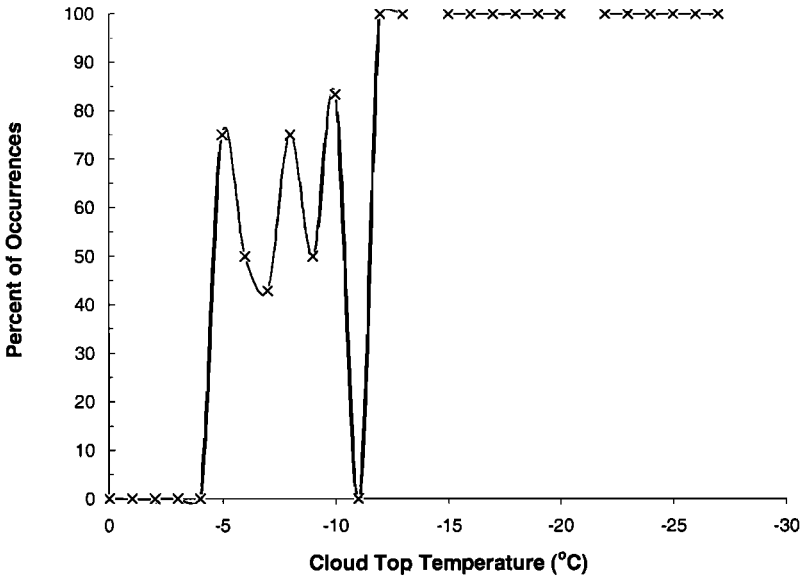

Figure 1. Frequency of occurrence of ice particles in arctic stratiform clouds versus cloud top temperature based on measurements obtained from the University of Washington Convair-580 research aircraft in 16 flights between May 19 and June 24, 1998.

The aircraft flight pattern in the line of broken stratocumulus cloud consisted of a gradual ascent at ~30 m per minute from cloud base (at 0.55 km mean sea level (msl) and 1°C) to cloud top (at 1.70 km msl and -6°C). At cloud top, aircraft penetrations were briefly made of what appeared to be the youngest cloud elements. The aircraft then descended to cloud base (at ~30 m per minute). The flight tracks were roughly along the length of the north-south-oriented line of stratocumulus cloud, with weaving to intercept the densest regions of the cloud. Both glaciated and mixed-phase cloud regions were sampled. The amount of ice found, and the absence of any ice-free regions, suggests that the clouds had passed the earliest stage of ice formation by the time the aircraft arrived. The lapse rate in the cloud was approximately pseudoadiabatic, indicating well-mixed clouds.

3. Instrumentation

The instrumentation aboard the Convair-580 for cloud microstructural measurements was the same as that described by *Hobbs and Rangno* [1998] but with the addition of the recently available SPEC Inc. Cloud Particle Imager or CPI [*Lawson and Jensen,* 1998]. The CPI can record up to 30 cloud particle images per second, and it resolves particles down to about 15 μm in maximum dimensions (MD). It can also record the size spectrum and concentrations of particles from ~5 to 2500 μm MD. For this study we used several thousand cloud particle images recorded by the CPI over a 25 min period when the Convair-580 was flying in the stratocumulus clouds on June 2, 1998. However, the CPI images were used only to classify and size the particles.

A possible source of error in the classification of the ice particles imaged by the CPI is that we may not have rejected enough particles as artifacts. The particles that we did reject as artifacts were similar particles (in size and shape) that showed up on a single frame. Sometimes there were more than 10 to 20 such particles. They appeared to be drops, frozen drops, or ice fragments. In the case to be described, the total number of particles of this type that were rejected was 220 (or about 7%) in the 25 min sample.

Another possible source of error is in the fragments. It is possible that the "unidentifiable fragments" we counted could have been produced by ice crystals shattering as they entered the CPI. However, it is known that snow particles at ground level often consist of a significant number of fragments [*Hobbs,* 1975].

Concentrations of ice particles referred to in this paper are from a Particle Measuring Systems (PMS) 2-D cloud probe. These concentrations are conservative estimates because they do not include ice particles <100 μm MD, nor have we corrected for the depth of field reduction for the 2-D probe for particles with MD between 100 and 150 μm.

Cloud liquid water contents were measured with a PMS Forward Scattering Spectrometer Probe (FSSP-100) and a Gerber PVM-100 probe. The liquid water contents from these probes were in very good agreement. Droplet concentrations and size spectra were measured with a FSSP-100 probe.

4. Results

Figure 2 shows some of the microphysical characteristics of the stratocumulus cloud studied on June 2, 1998. The spatial variabilities in droplet concentrations and liquid water content are apparent in Figures 2b and 2c. Figure 2d shows PMS 2-D cloud probe and CPI images of the ice particles in the cloud. The coincidence in several places of pockets of liquid water, with values near the maximum measured in these clouds, and high ice particle concentrations (>50 per liter) suggests that the ice had formed rather recently.

During the ~25 min (~130 km path length) that we flew in this stratocumulus cloud, ~3274 images of ice particles and water drops were imaged by the CPI. Of these, 2174 (66%) were ice particles. Table 1 shows an inventory of the ice particle types in this cloud. Fifty-three percent of the ice

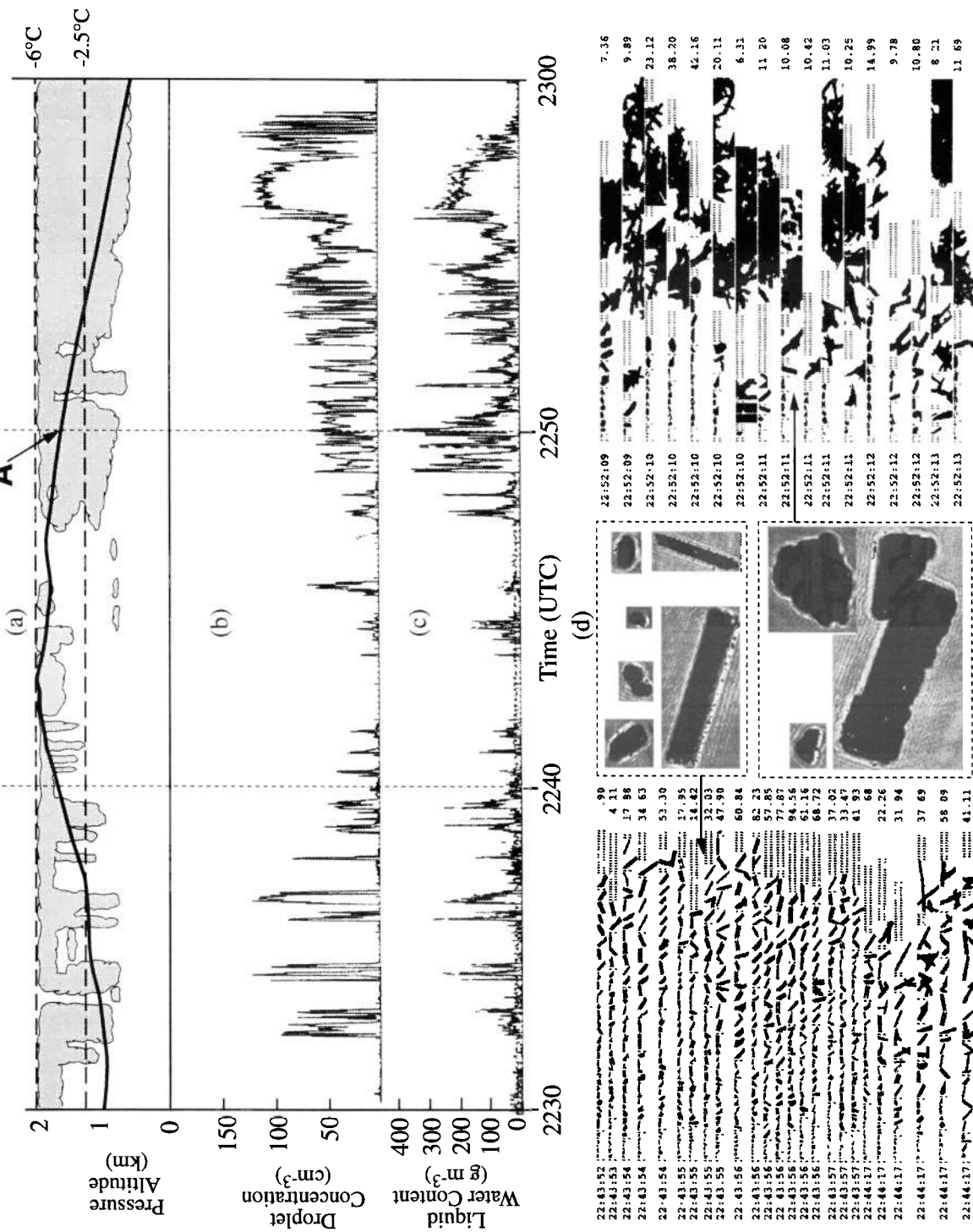

Figure 2. Cross section of cloud microphysical parameters measured during the ascent and descent of the University of Washington Convair-580 aircraft through the shallow, slightly supercooled stratocumulus cloud located near Barrow, Alaska, on June 2, 1998. (a) Aircraft flight track (solid line) through the cloud (shaded region). (b) Droplet concentrations from the PMS FSSP-100. (c) Liquid water content from the PMS FSSP-100 (solid line), and Gerber PVM-100 (dashed line). (d) Images of ice particles from the PMS 2-D cloud probe (left and right) and the SPEC CPI probe (center).

Table 1. Inventory of Ice Particle Types in the Stratocumulus Cloud on June 2, 1998

Particle Type	Number of Particles Imaged by CPI	Percentage of Total Particles	Number of Rimed Particles	Percentage of Rimed Particles
Irregularly shaped ice particles*	802	37	7	1
Frozen drops	424	20	0	0
Needles	386	18	105	27
Sheaths	184	8	20	11
Fragments of needles	174	8	67	39
Needles or sheaths	68	3	2	3
Short columns and plates	65	3	2	3
Fragments of sheaths	38	2	5	13
Aggregates	30	1	19	63
Graupel	3	0.1	3	100
Total ice particles imaged	2174			
Total rimed particles			230	11
Percentage of ice particles that were irregular or identifiable fragments		47		
Percentage of ice particles that were frozen drops		20		

Table refers to ice particles or crystals only. In addition, about 1100 water drops were imaged by the CPI.
*Does not include irregularly shaped particles that appeared to be fragments of regular ice crystal habits. Also, we do not include partially sublimated identifiable ice crystal habits in our definition of irregularly shaped ice particles.

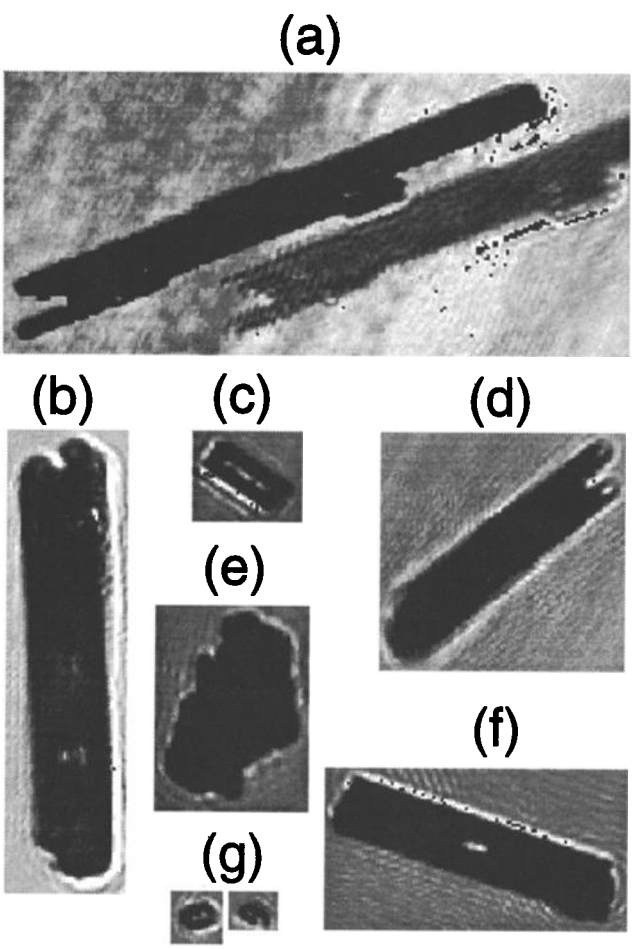

Figure 3. Examples of ice particle types imaged by the CPI for the arctic stratocumulus cloud studied on June 2, 1998. (a) Needle, (b) sheaths, (c) short column, (d) fragment of needle, (e) irregular ice particles, and (f) broken sheath, and (g) frozen drops (?).

particles were essentially intact and identifiable as either frozen drops (20%), needles or sheaths (29%), short columns and plates (3%), low-density aggregates (1%), or graupel (0.1%). Forty-seven percent of the ice particles were not pristine ice crystals; about one fifth of these particles were identifiable as fragments of needles and sheaths, the origins of the remaining four fifths of the nonpristine ice particles (called irregularly shaped) could not be discerned. About 11% of all the ice particles seen on the CPI were rimed. Figure 3 shows some examples of the ice particle types referred to above. We estimate that the percentage numbers of various ice particle types given above are correct to within about 5-10%.

In a recent publication, *Korolev et al.* [1999] reported that irregularly shaped particles accounted for about 97% of the ice they sampled in arctic clouds. However, their definition of irregular ice particles was much broader than ours, since it included partially sublimated and identifiable ice crystal habits with smooth sides as well as fragments with identifiable origins (see Korolev et al., Figure 2). If we had included these latter two types of ice particles in our "irregular" category, the percentage contribution from "irregularly shaped ice particles" would have been similar to that given by Korolev et al.

In the June 2, 1998, case, the greatest ice particle concentrations averaged over a 3 s time period (corresponding to a flight path through the cloud of ≈250 m) was 103 per liter. Over path lengths of 1 km the greatest average particle concentration was 85 per liter. Figure 4 compares the maximum ice particle concentration over 1 km for the June 2, 1998, case study with those measured by us in other arctic stratiform clouds in 1998. It can be seen from Figure 4 that maximum concentrations of ice particles well in excess of 10 per liter were quite common and that these high ice particle concentrations were essentially independent of cloud-top temperature from about –5° to –27°C. On the other hand, the lower limits to the maximum ice particle concentrations increase by about an order of magnitude per 10°C decrease in cloud-top temperature. All of the stratiform layers for which

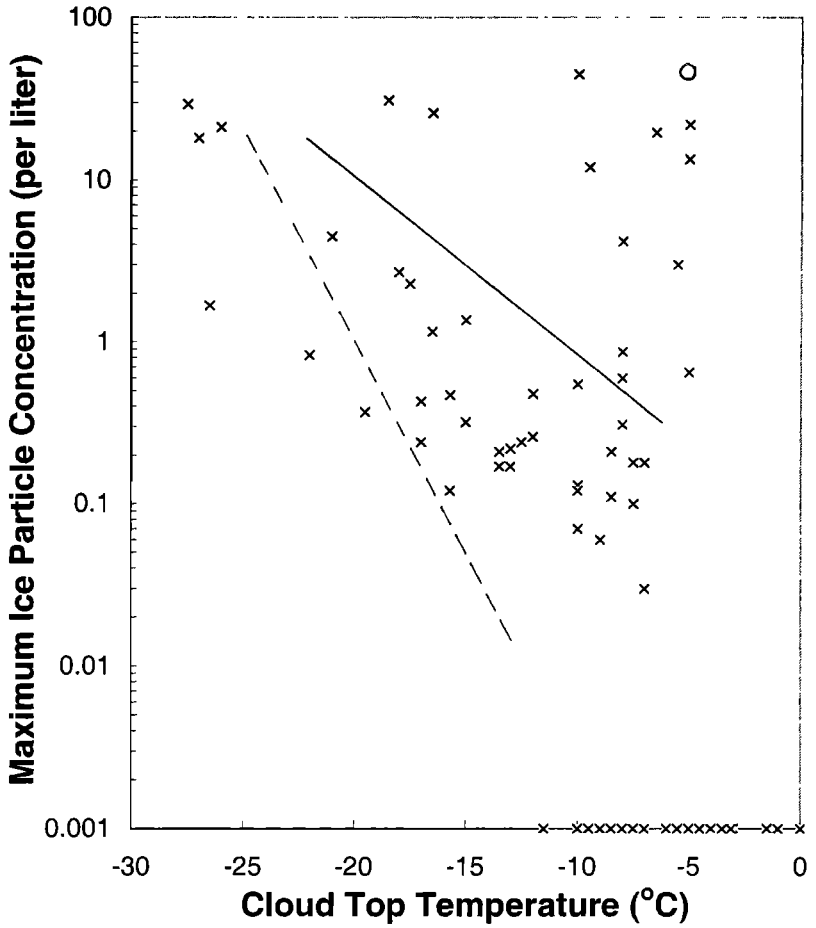

Figure 4. Maximum ice particle concentrations over 1 km path lengths versus cloud top temperature for altocumulus and stratocumulus clouds in the Arctic measured from the University of Washington Convair-580 aircraft in May and June 1998. The June 2 case study is shown by a circle. For comparison, the dashed line shows *Fletcher*'s [1962] summary of worldwide ice nucleus measurements, and the solid line is *Meyers et al.* [1992] summary of laboratory measurements of contact freezing ice nuclei.

data points are shown in Figure 4 (except the circle) had mainly liquid-phase cloud tops.

Ice particle concentrations in the slightly supercooled (–6°C) stratocumulus cloud on June 2 (the circle in Figure 4) were the highest observed in our 1998 study. This is consistent with the empirical results of *Hobbs and Rangno* [1985, 1998], who showed that the concentrations of ice particles in clouds increase sharply as the threshold diameter (D_T) of the cloud droplet spectrum increases (D_T is defined as the droplet diameter for which the cumulative concentration of droplets with diameters $>D_T$ is 3 cm^{-3}). Figure 5 shows maximum ice particle concentrations (over 1 km path lengths) versus D_T for all of the low- and middle-level arctic clouds sampled in 1998. It can be seen that the June 2 case had one of the highest D_T values (35 μm), and therefore, as predicted by the Hobbs-Rangno criterion, it had the greatest ice particle concentration in its aging portions.

Figure 4 shows, for comparison with our measurements of ice particle concentrations in arctic clouds, Fletcher's ice-nucleus-temperature relationship, which is a rough empirical fit to worldwide measurements and the somewhat higher ice nucleus concentrations given by *Meyers et al.* [1992] based on laboratory measurements of contact freezing using diffusion-type chambers. It is not known to what extent these curves, which are based on ice nucleus measurements at ground level and primarily in middle latitudes, are representative of ice nucleus concentrations in the Arctic, but it is unlikely that ice nucleus concentrations aloft in the Arctic exceed the values given by Meyers et al. It can be seen from Figure 4 that for cloud-top temperatures between about –10°C and –5°C, ice particle concentrations in arctic clouds can be about 1–2 orders of magnitude greater than the Meyers' curve. At cloud-top temperatures between –10°C and –18°C the ice particle concentrations can be about an order of magnitude greater than the maximum likely ice nucleus concentrations, and below about –20°C there appears to be no significant difference between ice nucleus and ice particle concentrations. In section 5, we will consider several possible mechanisms for the production of ice particle concentrations in excess of ice nucleus concentrations in arctic clouds.

5. Possible Mechanisms for High Ice Particle Concentrations in Arctic Clouds

Extensive documentation exists on ice particle concentrations well in excess of ice nucleus concentrations in various types of cloud outside of the Arctic [e.g., *Koenig*, 1963; *Mossop et al.*, 1967; *Hobbs*, 1969, 1975]. The recent

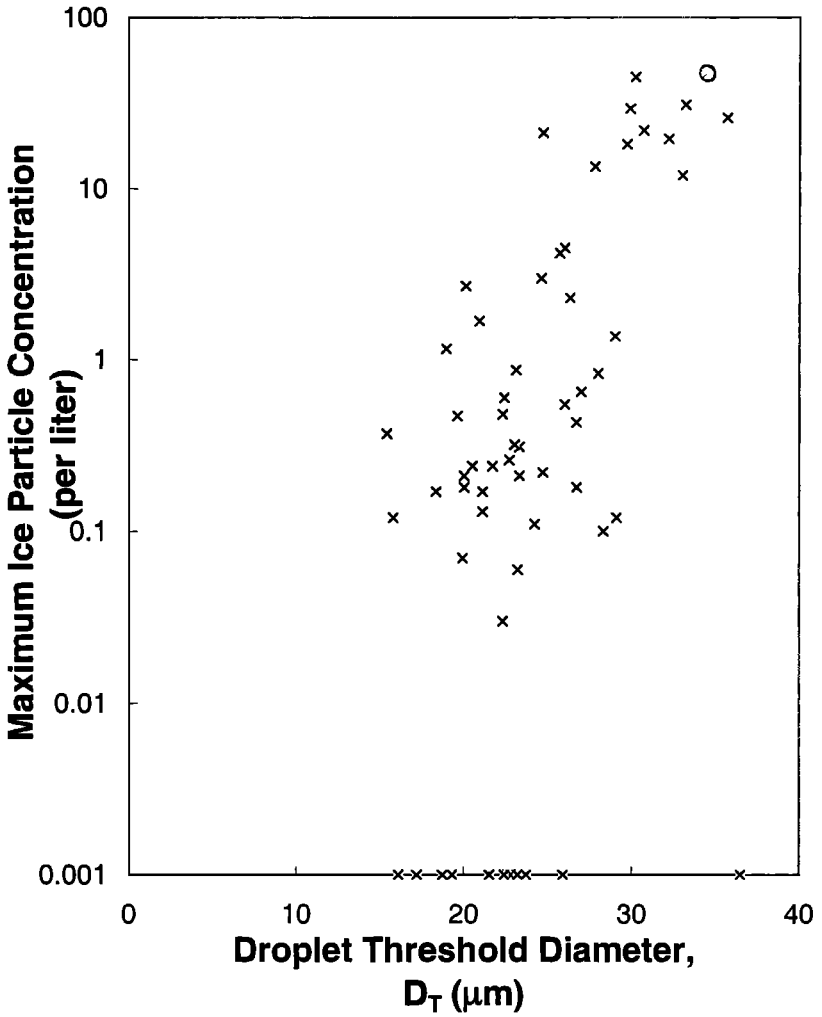

Figure 5. Maximum ice particle concentrations over 1 km path lengths versus the threshold diameter of the cloud droplet spectrum for the same data set shown in Figure 4.

report of *Hobbs and Rangno* [1998], as well as the present study (Figure 4), shows that high ice particle concentrations in clouds are also common in the Arctic. The relative simplicity of some arctic stratiform clouds, such as the case study described here, makes them particularly attractive for testing various mechanisms that have been proposed to explain ice enhancement. Moreover, the significant advancement in the quality of cloud ice particle imagery provided by the CPI provides important information for evaluating some of the proposed ice enhancement mechanisms.

In this section we use data from the June 2, 1998, case study to explore the applicability of four mechanisms that have been suggested to explain ice enhancement: ice splinter production during riming [*Hallett and Mossop*, 1974; *Mossop and Hallet*, 1974; *Mossop*, 1985], the shattering of isolated drops during freezing [*Hobbs and Alkezweeny*, 1968; *Brownscombe and Thorndyke*, 1968; *Bader et al.*, 1974; *Pruppacher and Schlamp*, 1975], fragmentation produced by the collision of ice crystals with each other and ice crystals with supercooled drops [*Hobbs and Farber*, 1972; *Vardiman*, 1978], and nucleation of ice at high water supersaturations adjacent to freezing supercooled drops [*Dye and Hobbs*, 1966; *Gagin and Nozyce*, 1984; *Fukuta and Lee*, 1986].

5.1. Riming-Splintering

The best quantified mechanisms for ice enhancement is the shedding of ice splinters during riming. For this to occur the supercooled droplets that collide with an ice particle must freeze approximately symmetrically inward so that liquid water is trapped beneath an ice shell. As this water freezes and expands, it exerts considerable pressure on the ice shell, which may consequently shatter into many ice splinters. Laboratory simulations of this process by *Hallett and Mossop* [1974], *Mossop and Hallet* [1974], and *Mossop* [1985] indicate that the necessary conditions for significant ice splinter production during riming are temperatures between −2.5° and −8°C, colliding supercooled droplets with diameters >23 μm present in concentrations >1 cm^{-3}, and impact speeds of ~0.2 to 5 m s^{-1}. About one in 200-250 droplets that rimed shed ice splinters in these laboratory studies.

The June 2 case study satisfied all three of the Hallett-Mossop (H-M) criteria in some very localized regions of the cloud. For example, the concentrations of droplets with diameters >23 μm reached a peak 1 s value of 28 cm^{-3} at −3.3°C, which means there were plentiful droplets to produce ice splinters during riming in small pockets of the cloud. For example, droplets of this size were present in concentrations

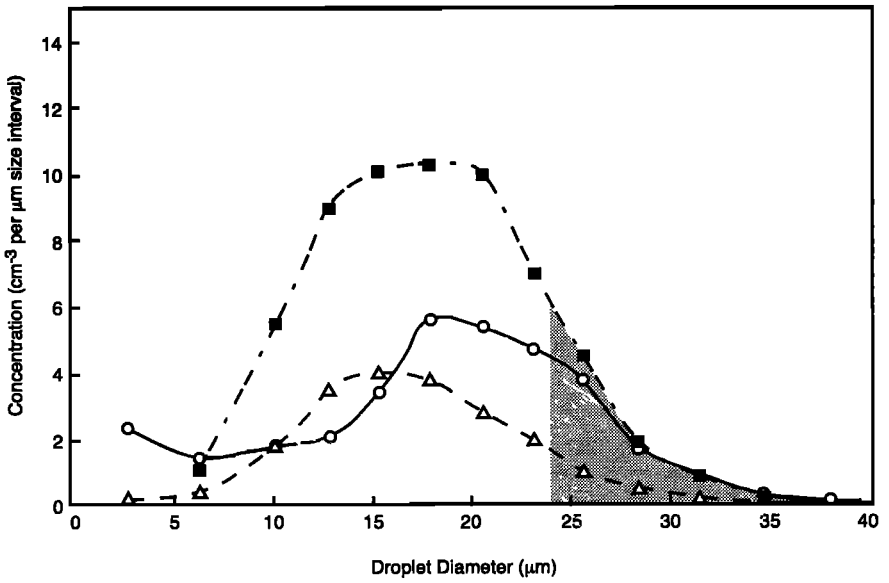

Figure 6. Average cloud droplet size spectrum measured with the PMS FSSP-100 probe in a region of mainly supercooled water (point A in Figure 2) at –3° to –6°C on June 2, 1998 (open circles). The shaded region indicates that portion of the drop size spectrum where about one in 200-300 rimed droplets would be expected to eject one ice splinter according to *Mossop* [1985]. The squares and triangles show the droplet size spectra in the laboratory clouds used by *Mossop* [1985] to measure ice splinter production produced during riming.

>1 cm^{-3} for only 173 s (or 22%) of the 13 min that the aircraft was in the temperature zone required for the H-M mechanism to operate. Figure 6 shows the droplet spectra in the region of the cloud where the liquid water content was highest (point A in Figure 2). For comparison, Figure 6 also shows the droplet size spectra in the laboratory experiments of *Mossop* [1985].

To estimate the rate of production of ice splinters by riming for the June 2 case study, we used *Mossop*'s [1985] laboratory results together with the cloud properties measured on June 2. Two categories of ice particles present in these clouds were considered to be rimers, namely, large columnar crystals (300-1000 µm MD) and quasi-spherical aggregates with an average MD of 1.5 mm. The reason for these choices is that the riming of pristine columnar crystals was observed in the CPI imagery to begin at about 300 µm maximum dimension. Also, all of the particles with MD >1 mm were aggregates. The collection efficiencies of the columnar crystals and aggregates for drops >23 µm diameter were taken to be 0.85 and 0.70, respectively [*Pruppacher and Klett*, 1997]. The flight data were averaged over horizontal slabs separated by temperature intervals of 0.5°C. The cloud microstructure was assumed to remain constant for 10 min, and the concentration of ice splinters produced in that time interval by riming in each region of the cloud was computed as follows:

The rate of splinter production per second was taken to be [*Willis and Hallett*, 1991]

$$\frac{N_g N_d V_g \pi D^2 E}{800},$$

where N_g is the concentration of riming ice particles per liter (in this case, single columnar ice crystals and their aggregates >300 µm MD), N_d is the concentration (cm^{-3}) of drops >23 µm diameter, V_g is the terminal fall velocity (m s^{-1}) of the riming ice particles (0.75 and 1.0 m s^{-1} for single columns and their aggregates, respectively), D is the diameter (in mm) of the riming particles (0.6 and 1.5 mm, respectively), and E is the collection efficiency (assumed 0.70 and 0.85, respectively, for single column and their aggregates). Following *Willis and Hallett* [1991] we assumed that one ice splinter was produced for every 200 drops rimed.

The results of the calculations are shown by the thin dashed line in Figure 7. No splinter production is indicated for temperatures below –5°C, because no droplets were measured in spite of an attempt to sample the youngest cloud portions near cloud top. Nevertheless, it can be seen from Figure 7 that the production of ice splinters by riming might well explain the high concentrations of ice particles measured in the stratocumulus cloud on June 2 and the high concentrations of ice particles between –4°C and –10°C in the other clouds for which data are shown in Figure 4. However, the ice particle imagery provided by the CPI for the June 2 case study casts possible doubt on whether this mechanism alone can explain the high ice particle concentrations in this temperature zone. This is because the small (µm or submicron) ice splinters produced by riming might be expected to grow rather quickly into pristine and identifiable ice crystal habits (such as needles or sheaths). Although such crystals were imaged by the CPI, they accounted for about 30% of the ice particles (Table 1). Instead, the ice particles were dominated by irregularly shaped ice particles and frozen drops (Table 1). The irregularly shaped ice particles had a modal size around 50 µm MD, and the diameters of the frozen drops were generally greater than 20 µm (Figure 8). This suggests that the shattering of relatively large isolated drops during freezing, and the mechanical fragmentation of large ice crystals, could have made important contributions to the large numbers of irregularly shaped ice particles. These two mechanisms are discussed in section 5.3.

Figure 4 also shows that at temperatures between about –10°C and –18°C, ice particle concentrations in arctic clouds

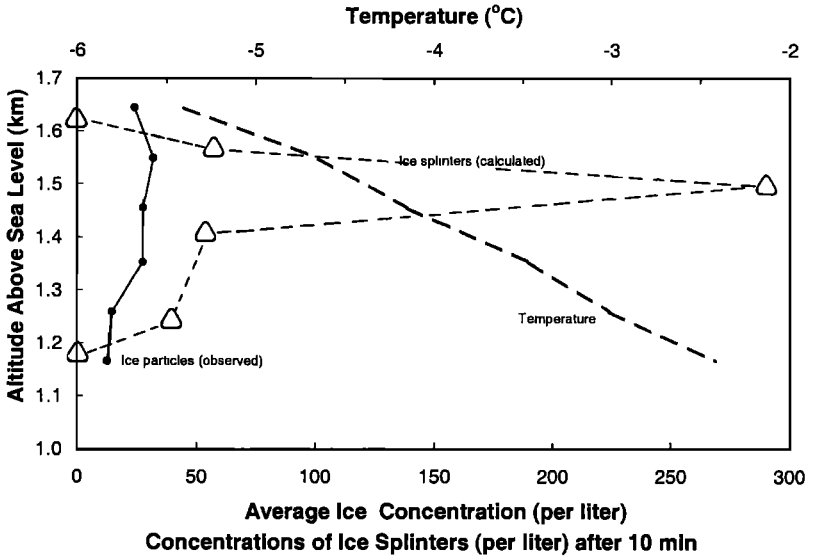

Figure 7. Vertical profiles of measured ice particle concentrations >100 μm MD (solid line) and average temperatures (thick dashed line) measured during the climb and descent of the aircraft on June 2, 1998. The thin dashed line shows computations of the concentrations of ice splinters (of unknown size) produced by riming after 10 min based on the laboratory experiments of *Mossop* [1985] and measured conditions in the arctic cloud on June 2, 1998 (see text for details).

can exceed ice nucleus concentrations by about a factor of 10. Since for our 1998 data set the clouds in this temperature category did not have any of their volume in the riming-splintering temperature zone (–2.5° to –8°C), the high ice particle concentrations in these clouds could not have been produced by riming-splintering. Also, there were no higher-level clouds to provide "seed" ice particles. Again, it is possible that the relatively high concentrations of ice particles in these clouds at temperatures between –10° and –18°C were produced by the fragmentation of ice crystals and/or the shattering of isolated drops as they froze in free fall.

5.2. Shattering of Isolated Drops During Freezing

Laboratory experiments have shown that as an isolated drop freezes, it may shatter into a number of relatively large irregularly shaped ice particles, as well as much smaller splinters [*Mason and Maybank,* 1960; *Dye and Hobbs,* 1966; *Hobbs and Alkezweeny,* 1968; *Brownscombe and Hallett,* 1968; *Griggs and Choularton,* 1983]. Shattering is favored for larger drops (>50 μm diameter) and when drops freeze approximately symmetrically inward. Since larger drops spin as they freeze in free fall [*Pruppacher and Schlamp,* 1975],

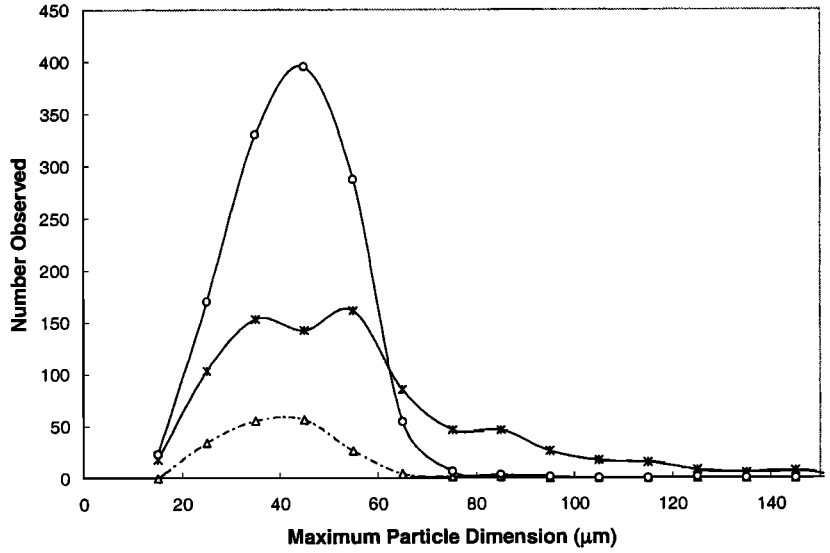

Figure 8. Number of liquid drops (circles), frozen drops (triangles), and irregularly shaped ice particles (asterisks) with maximum dimensions ≥ 20 μm from the CPI images for the 13 min that the Convair-580 flew between –2.5° and –6°C in the stratocumulus cloud on June 2, 1998.

they may freeze symmetrically and shatter. Also, if a supercooled drop is nucleated by a pointed extremity of an ice crystal, symmetrical freezing is probable [*Johnson and Hallett,* 1968].

In the June 2 case study, conditions were favorable for isolated drops to shatter during freezing. This is because large supercooled drops were present (Figure 8), and during freezing, these drops would probably have rotated in free fall, which increases the likelihood of shattering. Also, frozen drizzle drops preceded the formation of the high ice particle concentrations on June 2. Hence the large numbers of irregularly shaped ice particles in this cloud could have come in part from the large fragments produced by the shattering of isolated drops during freezing in free fall.

5.3. Fragmentation of Ice Crystals by Collisions

Thirty-seven percent of the ice particles in the June 2 case study were irregularly shaped ice particles (Table 1). Fragmentation of delicate crystals (such as dendrites and aggregates) may occur during crystal-crystal collisions and crystal-droplet collisions [*Hobbs and Farber,* 1972]. Although there were only a few aggregates of needles or sheaths, some of these exceeded 3 mm in size. As the aggregates fell through the cloud, they would have collided with many smaller crystals, which could have caused pieces of the aggregates to break off. For example, the average concentrations of aggregates in the vertical H-M layer was 2.2 per liter. The mean diameter of these aggregates was 1.5 mm, and the depth of the cloud to the freezing level was 900 m. Assuming a collection efficiency of 0.85 of single-columnar crystals by an aggregate, and conservatively assuming that the concentration of single (whole) columnar crystals was 10 per liter, the volume swept out by the aggregates (about 3.5 m^3) suggests that there would have been many thousands of collisions of aggregates with single-columnar crystals in the 900 m depth of subfreezing cloud. These collisions might account for the fact that the fragments of needles (particularly tips of needles) comprised the largest portion of the identifiable fragments (Table 1).

Hobbs and Farber suggested that during the riming process the thermal shock produced by the nucleation of supercooled drops might also cause delicate crystals to fragment. About 10% of the ice particles imaged by the CPI in the June 2 case study were identifiable as fragments of needles and sheaths (Table 1). While riming may not have played a large role in causing the fragmentation of the sheaths (since only about 13% of the sheath fragments were rimed), it could have been more important in the fragmentation of needles since nearly 40% of the fragments of needles were rimed. Also, the tips of needles were common as fragments, suggesting that they are particularly vulnerable to breaking off from their parent crystals.

It is, perhaps, significant that those clouds with relatively high particle concentrations at cloud-top temperatures between about –10°C and –18°C lie in the temperature regime when delicate ice dendrites grow.

5.4. Nucleation of Ice at High Water Supersaturations

Laboratory studies by *Dye and Hobbs* [1966] and *Gagin and Nozyce* [1984], as well as theoretical studies by *Fukuta and Lee* [1986], have shown that when a supercooled droplet freezes, there is a momentary burst of high supersaturation (>10%) in the air surrounding the drop, and this may lead to enhanced primary ice nucleation. *Hobbs and Rangno* [1990] and *Rangno and Hobbs* [1991] suggested that these high supersaturations might contribute to ice enhancement in polar maritime clouds. Since this process enhances ice formation on ice nuclei, it should produce small pristine ice crystals. However, as we have seen, small pristine ice crystals accounted for only about 32% of the ice particles in the June 2 case study (Table 1). While these crystals could have originated from primary ice nucleation, it is more likely that they grew from ice splinters produced by the riming and the shattering of isolated drops during freezing in free fall.

6. Summary and Conclusions

Slightly and moderately supercooled, boundary layer stratiform clouds, with low droplet concentrations, high ice particle concentrations, and drizzle drops are common in the Arctic in late spring and summer. In this paper we have described such a case, which is typical of this type of cloud, and we have discussed some possible mechanisms for the production of ice particle concentrations significantly greater than ice nucleus concentrations.

For those clouds that encompass temperatures between about –2.5°C and –8°C, ice splinter production during riming appears capable of explaining the high ice particle concentrations. However, in view of the relatively large sizes (>40 μm MD) and irregular shapes of the majority of the ice particles (Table 1), this would require that the tiny splinters produced by riming grow into irregular particles. The numerous large and irregularly shaped ice particles could have been produced by the shattering of drops >50 μm diameter during freezing in free fall and the fragmentation of delicate ice crystals during collisions. These latter two mechanisms could also be responsible for the high ice particle concentrations (>10 L^{-1}) in arctic stratiform clouds with top temperature between about –10°C and –18°C (Figure 4) and which lie outside of the zone where splinter production due to riming can occur.

Figure 9, which is based on information presented here and in an earlier study of arctic clouds [*Hobbs and Rangno,* 1998], shows in schematic form the microstructures of slightly supercooled (top temperatures –4°C to –10°C) and moderately supercooled (top temperatures –10°C to –20°C) stratiform clouds in the Arctic and the various processes that appear to be responsible for the production of high ice particle concentrations in these clouds. The picture that emerges is consistent with that which we have described previously for low- and middle-level stratiform clouds in temperate latitudes, namely that the amount of ice issuing from such clouds is strongly dependent on the largest cloud droplets generated in the clouds (e.g., Figure 5 in this paper, and *Hobbs and Rangno* [1985, 1998]). For the development of drizzle and, subsequently ice, in slightly supercooled clouds, the presence of droplets with diameters greater than about 28 μm is necessary. At temperatures above –4°C, ice does not appear to be able to form in these clouds regardless of droplet size.

Slightly supercooled stratus or stratocumulus cloud of the Type 1 variety (Figure 9a) are of limited depth and contain relatively high droplet concentrations (>100 cm^{-3}). Therefore they do not contain droplets >28 μm diameter, which are necessary for the formation of drizzle, and they contain very

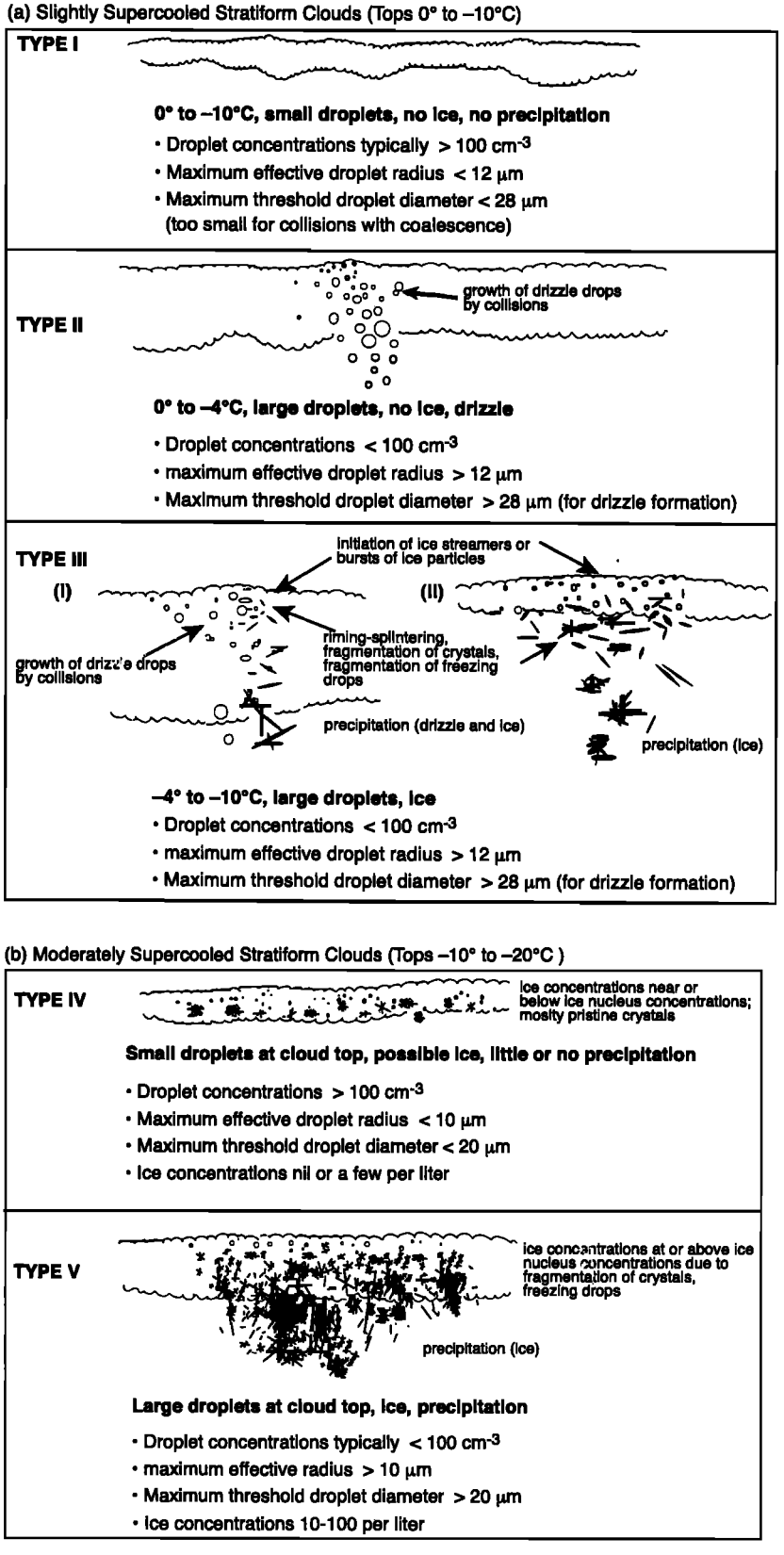

Figure 9. Schematic depiction of the structures and mechanisms for forming ice in (a) slightly, and (b) moderately supercooled, stratiform clouds in the Arctic.

little, if any, ice. Since these clouds may contain droplets >23 μm diameter, ice splinter production during riming could occur if ice particles were introduced into the clouds by, for example, falling into the cloud from above. Otherwise these clouds do not precipitate either drizzle or ice particles.

Slightly supercooled stratiform clouds of the Type II and Type III variety (Figure 9a) contain droplets with diameters >28 μm and thus have a propensity for drizzle formation, and if their top temperatures are below –4°C, they will probably generate high concentrations of ice particles. The liquid tops of these ice-producing clouds are often punctuated with extremely localized (tens to a few hundred of meters in width) bursts of freshly initiated ice particles [*Hobbs and Rangno*, 1998]. These bursts of ice are probably the upper portions of vertical ice streamers (seen, for example, on 35 GHz radar displays [*Hobbs et al.*, this issue]).

The mechanisms for the formation of ice concentrations greatly in excess of ice nuclei in slightly supercooled stratiform clouds in the Arctic appear to be ice splinter production when a few frozen drizzle drops begin to rime; the fragmentation of drizzle-size drops as they freeze; and the fragmentation of existing delicate ice crystals.

The formation of high ice particle concentrations in moderately supercooled stratiform clouds (Figure 9b) is also dependent on the largest droplet sizes in the cloud, but the dependence is less spectacular than for slightly supercooled clouds. Type IV clouds contain only small droplets (≤20 μm diameter), because they are either very thin or droplet concentrations are elevated; also, at these lower temperatures the supply of vapor is limited. In the Arctic, few ice particles form in such clouds. When the droplets attain larger sizes, due to either low droplet concentrations and/or greater cloud thickness, higher concentrations of ice particles can form by the fragmentation of delicate ice crystals and the freezing of drops (Type V).

Acknowledgments. This research was supported by grant NAG1-2079 from the NASA Radiation Program and grant OPP-9808163 from the National Science Foundation Arctic Sciences Section. Partial support for the UW Convair-580 research facility is provided by NASA Cooperative Agreement NCC5-326.

References

Bader, M., J. Gloster, J. L. Brownscombe, and P. Goldsmith, The production of sub-micron ice fragments by water droplets freezing in free fall or on accretion upon an ice surface, *Q. J. R. Meteorol. Soc., 100,* 420-426, 1974.

Brownscombe, J. L., and J. Hallett, Experimental and field studies of precipitation particles formed by the freezing of supercooled water, *Q. J. R. Meteorol. Soc., 94,* 455-473, 1968.

Brownscombe, J. L., and N. S. C. Thorndyke, The freezing and shattering of water droplets in free fall, *Nature, 220,* 687-689, 1968.

Curry, J. A., E. E. Ebert, and J. L. Schramm, Impact of clouds on the surface radiation balance of the Arctic Ocean, *Meteorol. Atmos. Phys., 51,* 197-217, 1993.

Curry, J. A., W. B. Rossow, D. Randall, and J. L. Schramm, Overview of arctic cloud and radiation characteristics, *J. Clim., 9,* 1731-1759, 1996.

Dye, J. E., and P. V. Hobbs, The effect of carbon dioxide on the shattering of freezing drops, *Nature, 209,* 464-466, 1966.

Fletcher, N. H., *Physics of Rain Clouds*, 386 pp., Cambridge Univ. Press, New York, 1962.

Fukuta, N., and H. J. Lee, A numerical study of the supersaturation field around growing graupel, *J. Atmos. Sci., 43,* 1833-1843, 1986.

Gagin, A., and H. Nozyce, The nucleation of ice crystals during the freezing of large supercooled drops, *J. Rech. Res., 7,* 870-874, 1984.

Griggs, D. J., and T. W. Choularton, Freezing modes of riming droplets with application to ice splinter production, *Q. J. R. Meteorol. Soc., 109,* 243-253, 1983.

Hallett, J., and S. C. Mossop, Production of secondary particles during the riming process, *Nature, 249,* 26-28, 1974.

Hobbs, P. V., Ice multiplication in clouds, *J. Atmos. Sci., 26,* 315-318, 1969.

Hobbs, P. V., The nature of winter clouds and precipitation in the Cascade Mountains and their modification by artificial seeding, part I, Natural conditions, *J. Appl. Meteorol., 14,* 783-804, 1975.

Hobbs, P. V., and A. J. Alkezweeny, The fragmentation of freezing water drops in free fall, *J. Atmos. Sci., 25,* 881-888, 1968.

Hobbs, P V., and R. Farber, Fragmentation of ice particles in clouds, *J Res. Atmos., 6,* 245-258, 1972.

Hobbs, P. V., and A L. Rangno, Ice particle concentrations in clouds, *J. Atmos. Sci., 42,* 2523-2549, 1985.

Hobbs, P. V., and A. L. Rangno, Rapid development of ice particle concentrations in small polar maritime clouds, *J. Atmos. Sci., 47,* 2710-2722, 1990.

Hobbs, P. V, and A. L. Rangno, Microstructures of low and middle-level clouds over the Beaufort Sea, *Q J. R. Meteorol. Soc., 124,* 2035-2071, 1998.

Hobbs, P. V , A. L. Rangno, T. Uttal, and M. Shupe, Airborne studies of cloud structures over the Arctic Ocean and comparisons with retrievals from ship-based 35 GHz radar and radiometer measurements, *J. Geophys. Res.*, this issue.

Johnson, D. A., and J. Hallett, Freezing and shattering of supercooled water drops, *Q. J. R. Meteorol. Soc., 94,* 468-482, 1968.

Koenig, L. R., The glaciating behavior of small cumulonimbus clouds, *J. Atmos. Sci., 20,* 29-47, 1963.

Korolev, A. V., G. A. Isaac, and J. Hallett, Ice particle habits in arctic clouds, *Geophys. Res. Lett, 26,* 1299-1302, 1999.

Lawson, R. P., and T. L. Jensen, Improved microphysical observations in mixed phase clouds, in *Preprints of the AMS Conference on Cloud Physics,* pp. 451-484, Am. Meteorol. Soc., Boston, Mass., 1998.

Mason, B. J., and J. Maybank, The fragmentation and electrification of freezing water drops, *Q. J. R. Meteorol. Soc., 86,* 176-186, 1960.

Meyers, M. P , P. J. DeMott, and W. R. Cotton, New primary ice-nucleation parameterizations in an explicit cloud model, *J. Appl. Meteorol., 31,* 708-721, 1992.

Mishchenko, M. I., W. B. Rossow, A. Macke, and A. A. Lacis, Sensitivity of cirrus cloud albedo, bidirectional reflectance and optical thickness retrieval accuracy to ice particle shape, *J. Geophys. Res , 101,* 16,973-16,985, 1996.

Mossop, S C., Secondary ice particle production during rime growth: The effect of drop size distribution and rimer velocity, *Q. J. R. Meteorol. Soc., 111,* 1113-1124, 1985.

Mossop, S. C., and J. Hallett, Ice crystal concentration in cumulus clouds: Influence of the drop spectrum, *Science, 186,* 632-633, 1974.

Mossop, S. C., A. Ono, and J. K. Heffernan, Studies of ice crystals in natural clouds, *J. Res. Atmos., 1,* 45-64, 1967.

Pruppacher, H. R., and J. D. Klett, *Microphysics of Clouds and Precipitation,* 2nd ed., 954 pp., Kluwer Acad., Norwell, Mass., 1997.

Pruppacher, H. R., and R. J. Schlamp, A wind tunnel investigation on ice multiplication by freezing of water drops falling at terminal velocity in air, *J. Geophys. Res., 80,* 380-385, 1975.

Rangno, A. L., and P. V. Hobbs, Ice particle concentrations and precipitation development in small polar maritime cumuliform clouds, *Q. J. R. Meteorol. Soc., 117,* 207-241, 1991.

Vardiman, L., The generation of secondary ice particles in cloud crystal-crystal collisions, *J. Atmos. Sci., 35,* 2168-2180, 1978.

Willis, P. T., and J. Hallett, Microphysical measurements from an aircraft ascending with a growing isolated maritime cumulus tower, *J. Atmos. Sci., 48,* 203-300, 1991.

P. V. Hobbs and A. L. Rangno, Department of Atmospheric Sciences, University of Washington, Box 351640, Seattle, WA 98195-1640. (phobbs@atmos.washington.edu; art@atmos.washington.edu)

(Received December 17, 1999; revised April 24, 2000; accepted May 4, 2000)